Chapter 1

Introduction and Literature Review

This chapter presents a brief overview of global energy consumption and future energy demand driven by present non-renewable energy sources, along with the necessity for viable alternatives to fossil fuels and a comprehensive overview of electrochemical water splitting. This chapter further includes brief survey of current state-of-the-art electrocatalysts utilized for electrochemical water splitting and also provides several strategies used to enhance the electrocatalytic activity towards HER and OER of transition metal oxide-based working electrodes.

1.1 Energy Demand and Need for Alternative Sources of Energy

In the last century, there has been an immense and fast increase in worldwide energy consumption, mostly driven by globalization and rising populations. The projected energy demand is expected to rise from 16 Terawatt (TW) in 2010 to 23 TW in 2030, with a potential increase to 30 TW by 2050. [1] Currently, fossil fuels provide more than 80% of the energy needed worldwide. In 2022, 82% of the world's primary energy usage provided by fossil fuels, which include oil (31.6%), coal (26.7%) and natural gas (23.5%) (**Figure 1.1)**. [2] On the other hand, renewable energy sources are only about ~14 % of all the natural resources, as depicted in **Figure 1.1**.

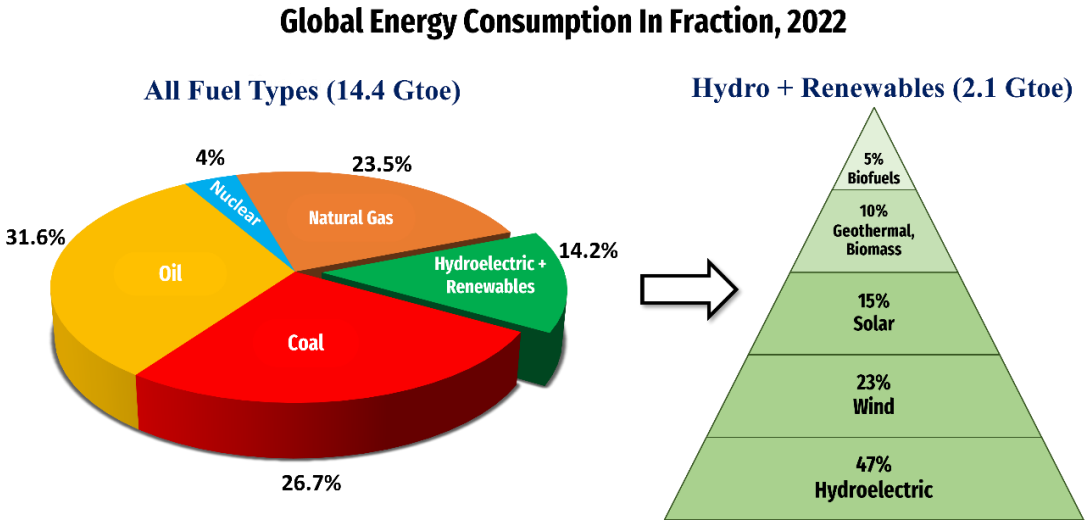

Figure 1.1 The world total primary energy consumption by fuels in 2022. [2]

The heavy reliance on fossil fuels has led to their depletion and environmental issues like global warming. As the fossil fuel reserves are fixed, sooner or later it will be exhausted, increased sophisticated extraction techniques like offshore drilling and fracking may defer the time of depletion. Industrialization and urbanization have caused a rise in greenhouse gases such as CO_2, NO_x and SO_x, which contribute to climate change. Fossil fuel combustion, especially coal burning, is the primary source of CO_2 emissions, [3] as depicted in **Figure 1.2**.

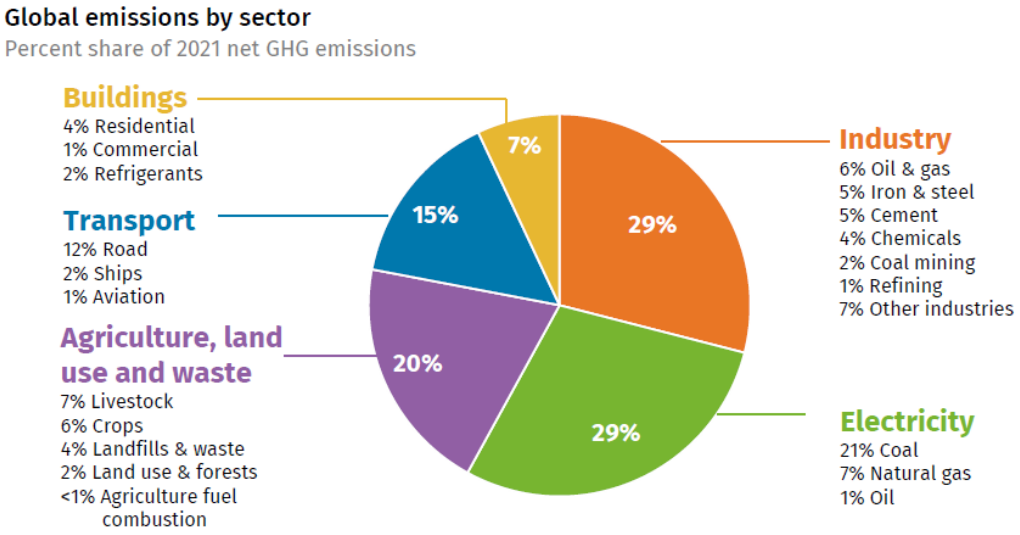

Figure 1.2 Global distribution of GHG emissions by different sectors. [3]

Therefore, it is essential to promote the advancement of renewable and environment friendly alternatives (such as solar, wind, tidal etc.) that are currently being utilized on a large scale. Nonetheless, these energy sources display intermittent characteristics, leading to energy wastage if not utilized or stored effectively. Consequently, there is a need for a clean fuel that is devoid of carbon and has the ability to store intermittent energy. Hydrogen stands out as a zero-emission fuel, seen as the cornerstone of renewable energy sources, facilitating the development of the hydrogen economy. Hydrogen presents a significant advantage compared to alternative fuels due to its impressive energy density of 143 GJ/tonne. [4]

1.1.1 Hydrogen as a Fuel

Molecular hydrogen gas (H_2) stands out as a most appealing fuel option. H_2 serves as an excellent energy carrier and stands as a potential candidate for future low-carbon energy systems, given its superior gravimetric energy density and the absence of pollutants during combustion. [5] To successfully achieve the hydrogen economy, it is crucial to develop a clean, renewable and efficient method for producing H_2 that does not introduce new challenges. [6]

Currently, approximately 96% of global hydrogen production derives from fossil fuels, specifically natural gas (43%), crude oil (32%), coal (20%) and 1% from biomass primarily through steam reforming. On the other hand, only around 4% of hydrogen is produced via water electrolysis, as depicted in **Figure 1.3**. [7-8]

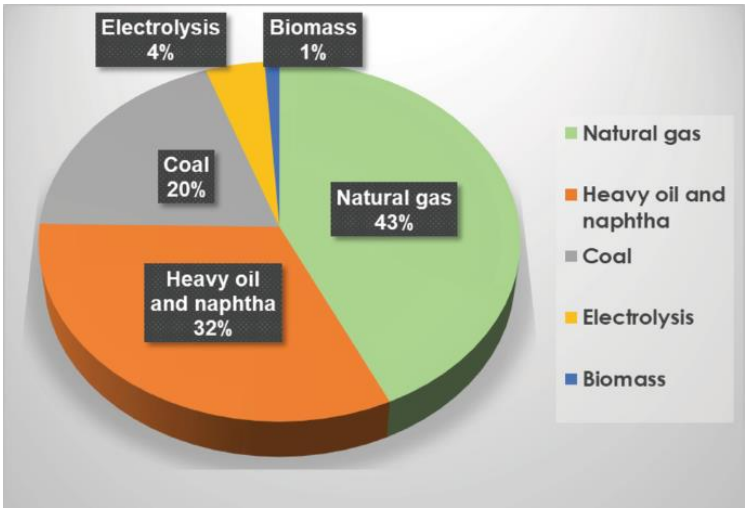

Figure 1.3: Hydrogen production through different sources. [9]

To mitigate CO_2 emissions and attain energy independence from fossil fuels, it is essential to significantly enhance the share of hydrogen produced from renewable sources in the next decades. Water electrolysis is an essential method that employs renewable energy to dissociate water into hydrogen and oxygen. Increasing the share of renewable energy from wind turbines or solar photovoltaic panels, along with the implementation of equitable CO_2 emission pricing, will enhance the attractiveness of hydrogen synthesis through water electrolysis. Integrating water electrolysis with renewable energy provides substantial advantages, as excess electrical energy can be chemically stored as hydrogen to mitigate the imbalance between energy demand and production. [10-11] The generated hydrogen gas can be stored and applied in industrial contexts, or employed for power generation through fuel cells or internal combustion engines, leading to zero CO_2 emissions. A sustainable approach for the circulation of a hydrogen economy through the integration of renewable energy and electrochemical water splitting depicted in **Figure 1.4**. Moreover, water electrolysis produces highly pure oxygen, applicable in various sectors such as healthcare and the chemical industry.

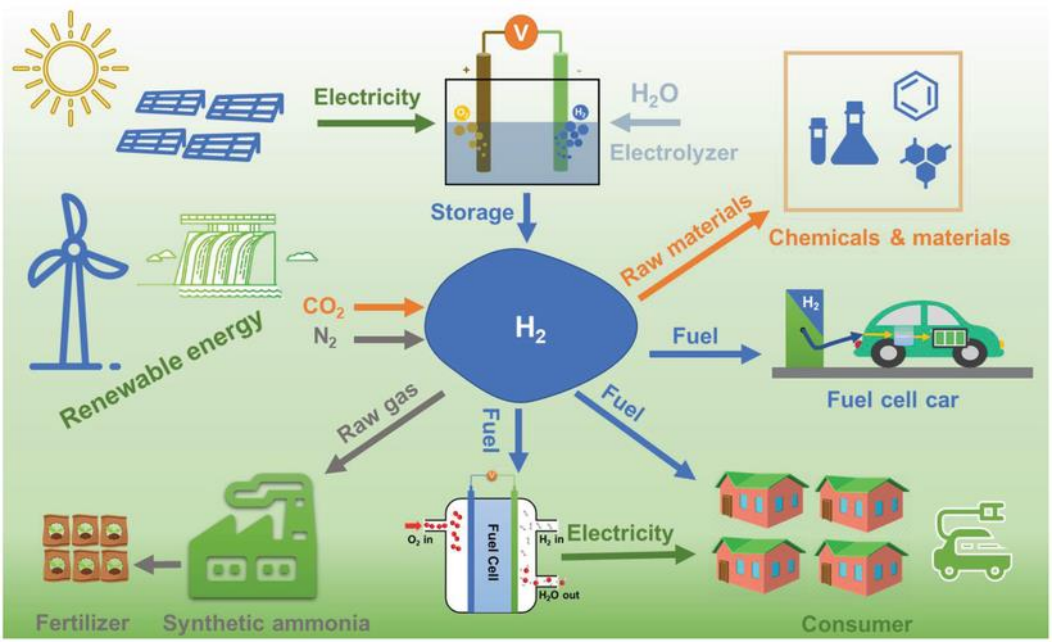

Figure 1.4 A sustainable pathway for the circulation of a hydrogen economy by combining renewable energy and electrochemical water splitting. [12]

1.1.2 Electrocatalytic Water Splitting and Need for Non-Noble Metals-Based Catalysts

Water electrolysis is an effective method for generating high-purity hydrogen without carbon emissions. The electrolysis cell for water splitting comprises three components: an anode, a cathode and an aqueous electrolyte. The process consists of two half-cell reactions: the reduction of water at the cathode, known as the hydrogen evolution reaction (HER) and the oxidation of water at the anode, referred to as the oxygen evolution reaction (OER). Since water is stable and not very conductive, conductive electrolytes like 0.5 M H_2SO_4 or 1 M KOH are generally utilized. [13] Electrocatalytic water splitting takes place in a cell that comprises two separate electrodes (**Figure 1.5**) under varying electrocatalytic conditions, mainly in basic and acidic environments. The reaction sequences in acidic and basic solutions differ, [14, 15] as illustrated in the following chemical equations,

Water Splitting Overall Reaction: $2H_2O\ (l)\ \rightarrow\ 2H_2(\mathrm{g}) + \ O_2(\mathrm{g})$ (1.1)

In acidic electrolyte:

Cathode (Reduction): $2H^+ + 2e^- \rightarrow H_2(\mathrm{g})$ (1.2)

Anode (oxidation): $2H_2O\ (l)\ \rightarrow O_2 + 4H^+ + 4e^-$ (1.3)

In alkaline electrolyte:

Cathode (Reduction): $2H_2O\ (l) + 2e^-\ \rightarrow H_2 +\ 2HO^-$ (1.4)

Anode (oxidation): $4HO^-\ \rightarrow\ O_2(\mathrm{g}) + 2H_2O\ (l) +\ 4e^-$ (1.5)

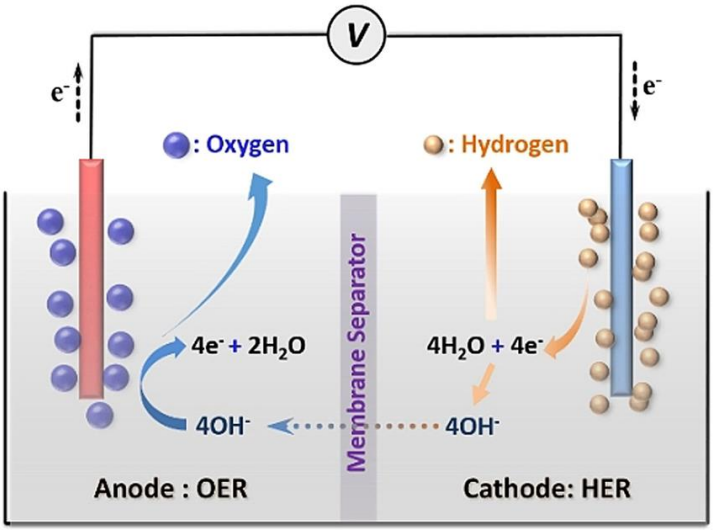

Figure 1.5: A typical water electrolysis cell under alkaline conditions. [16]

A minimum thermodynamic potential of 1.23 V *vs.* RHE is necessary to facilitate water splitting at 25 °C and 1 atm, regardless of the reaction medium in which the entire process takes place. The slow kinetics at the electrode interfaces mean that both the HER and the OER necessitate a significantly elevated potential to enable water splitting, making it essential to have an effective catalyst to minimize the additional potential needed. [16, 17]

Currently, the most effective electrocatalysts consist of noble-metal-based materials, specifically Pt and its derivatives for hydrogen evolution reactions, as well as Ir and Ru oxides for oxygen evolution reactions. The development of stable, highly active, earth-abundant and inexpensive electrocatalysts that are free from noble metals is critically needed for HER and OER due to their scarcity. [18, 19] The use of non-noble metal-based catalysts is expected to reduce overpotential, improve stability, enhance efficiency and boost OER kinetics. [20, 21]

Recent findings enabled the successful utilization of Iron group metals like Fe, Co and Ni and they were mostly explored as oxides, [22] hydroxides, [23] phosphides [24] and chalcogenides [25] for OER and HER at different pH conditions. However, the researchers continue to find that OER in acidic electrolytes is a bottleneck. Consequently, total water splitting under alkaline conditions using various 3*d* transition metal-based catalysts demonstrated significant results, with enhanced activity achievable through innovative surface modifications at the nanoscale. Literature analysis showed a significant utilization of earth-abundant electrocatalysts for applications in both the oxygen evolution reaction and the hydrogen evolution reaction. Electrocatalysts based on transition metals are synthesized through various methods, including oxides, hydroxides, chalcogenides, phosphides and layered double hydroxide (LDH) configurations, often in combination with other transition metal catalysts, tailored for both OER and HER under specific pH conditions. The results of transition metal-based catalysts demonstrate their potential in water splitting applications, which can be further improved through various effective approaches. Therefore, materials based on transition metals are in high demand for use as catalysts in the process of electrocatalytic water splitting.

1.1.2.1 Hydrogen Evolution Reaction (HER)

The hydrogen evolution reaction serves as the cathodic half-reaction in the process of water splitting. It involves a multi-step mechanism characterized by two-electron transfer occurring on the cathode surface, which can proceed through two different mechanisms, leading to three possible reactions, as shown in **Figure 1.6**. [26]

In these reactions, S stands for the catalyst surface and H* represents the absorbed hydrogen intermediate.

In the acidic electrolyte, the following steps are included in the HER process: [27]

(1) A proton from hydronium cation (H_3O^+) is captured by an electron from the catalyst surface, resulting in the adsorbed hydrogen intermediates (H*) on the catalytic surface.

$$H_3O^+ + e^- + S \rightarrow H^* + H_2O \,, Volmer\ reaction \tag{1.6}$$

(2) The adsorbed hydrogen atom couple with a proton and an electron simultaneously to generate hydrogen molecule.

$$H^* + H_3O^+ + e^- \rightarrow 2H_2 \,, Heyrovsky\ step \tag{1.7}$$

(3) Followed by a combination of adsorbed species to form H_2 gas:

$$H^* + H^* \rightarrow H_2, Tafel\ reaction \tag{1.8}$$

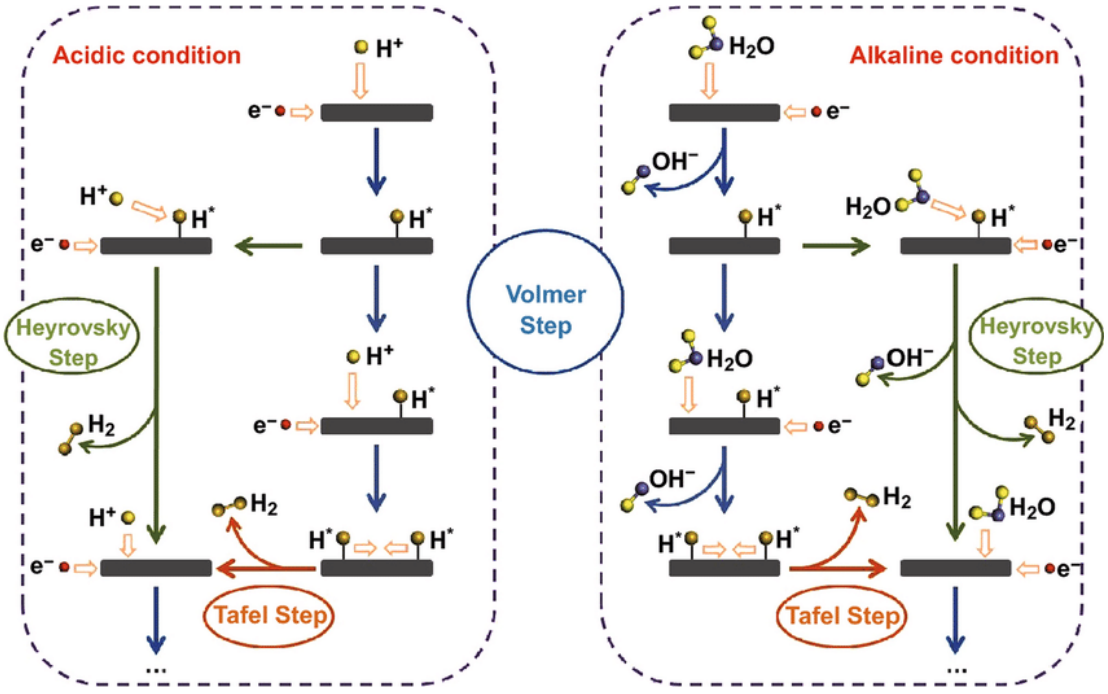

Figure 1.6 Schematic illustration of HER pathways in acidic and alkaline solutions. [28]

In contrast, in the alkaline electrolyte, HER proceeds via Volmer and Heyrosky reactions: [29]

(1) A proton from water molecule (H_2O) instead of hydronium cation (H_3O^+) combines with an electron to form the adsorbed hydrogen intermediate (H*)

$$H_2O + e^- + S \rightarrow H^* + OH^-, Volmer\ reaction \quad (1.9)$$

(2) The adsorbed hydrogen atom attracts a water molecule and an electron simultaneously to generate a hydrogen molecule.

$$H^* + H_2O + e^- \rightarrow H_2 + OH^-, Heyrovsky\ step \quad (1.10)$$

(3) As the same as the case of the acidic conditions, two absorbed hydrogen atoms are joined together chemically to generate a hydrogen molecule

$$H^* + H^* \rightarrow H_2,\ Tafel\ reaction \quad (1.11)$$

1.1.2.2 Oxygen Evolution Reaction (OER)

The process of OER at the anode involves a multistep four-electron transfer mechanism, which is inherently more complex compared to the HER occurring at the cathode. The mechanisms and reaction pathways of OER are comparatively more complicated than those of HER, largely due to the sluggish kinetics involved. In the acidic electrolyte, water undergoes oxidation to produce oxygen and hydrogen ions, while in the neutral or alkaline electrolyte, the hydroxyl ion is oxidized to yield water and oxygen. These possible OER mechanisms usually involve three adsorbed intermediates OH*, O* and OOH* on the catalyst surface (see **Figure 1.7**). [30] The major difference in the first elementary steps of OER in acid and in alkali is the adsorption of water and hydroxide ion on the surface-active site S. All elementary steps are related to the kinetic barriers, so it increases the overall overpotential of OER. The slowest sluggish kinetic elementary step is the rate-determining step (RDS).

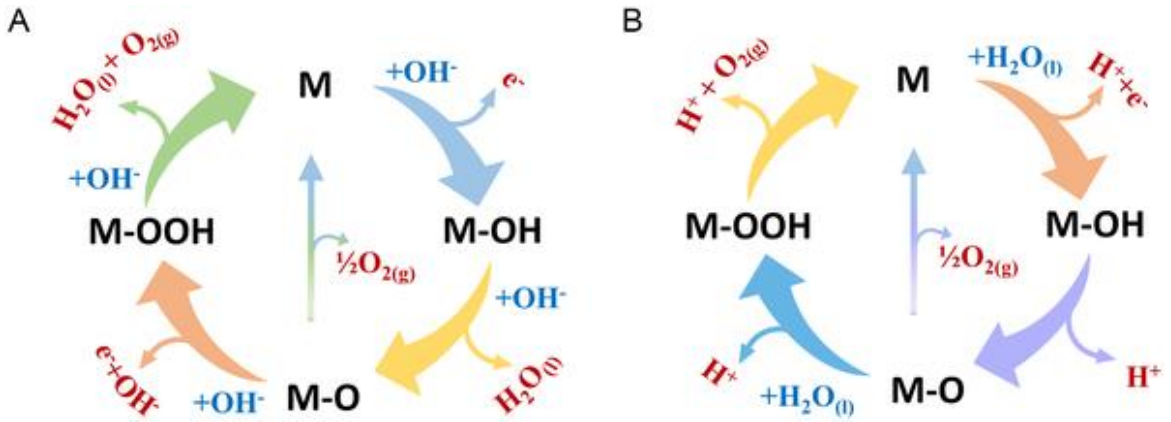

Figure 1.7: OER mechanism (A) in alkaline and (B) in acidic media. [31]

Two different methods are involved for oxygen production through MO intermediate. **Figure 1.7a, b** illustrates the two possible approaches for OER through MO intermediate in both the acidic and alkaline conditions respectively. Here, M stands for metal atoms. First, the oxygen is directly produced as a result from the combination of two MO molecules. Second, oxygen generation through MOOH intermediate formation, taking place toward decomposition, including acidic as well as basic mechanism. [31]

The mechanism of the oxygen evolution reaction involves the formation of several intermediates, making it difficult to identify the exact reaction pathway. In all the elementary steps, a common aspect is that the active site S experiences a cycle of oxidation and reduction reactions during the oxygen evolution reaction in both acidic and alkaline conditions. This occurs across all proposed mechanisms to produce O_2 molecules and restore the surface sites for the next cycle. Therefore, metals having stable and variable oxidation states work as effective catalysts for OER. This is why Ir and Ru are good electrocatalysts for OER in acidic media and the oxides and hydroxides of Ni, Co, Fe and Mn work well in alkaline conditions. [32, 33] Other than this, the catalytic activity depends on a few other significant characteristics of the catalyst in addition to a favorable electronic configuration and variable oxidation states. One important requirement is appropriate bond strength of the intermediates formed in the

elementary steps. The Sabatier principle states, an effective catalyst should bind the reactant (intermediate species) neither too strongly nor too weakly because these conditions result in inadequate reactant adsorption or difficulties removing end products, respectively as illustrated in **Figure 1.8**. [34, 35]

The catalyst surface must provide favorable conditions for reaction intermediates to be adsorbed. Hence, catalysts at the top of the Volcano plot are very good electrocatalysts (**Figure 1.9**).

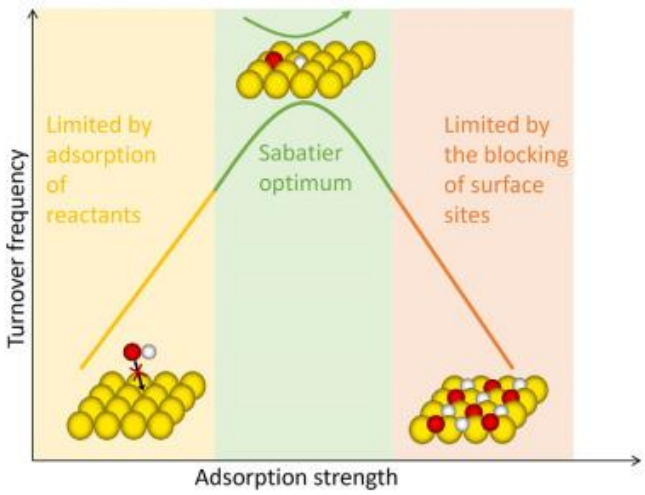

Figure 1.8. Qualitative schematic of the Sabatier principle. For strong-binding materials, the reaction is limited by slow formation or desorption of products. For weak-binding materials, the reaction is limited by slow adsorption or activation of reactants. Thus, the optimal catalyst features an intermediate binding strength. [36]

1.1.3 Noble-Metal Based Catalysts for OER and HER

Noble metals such as Ir, Ru, Pd, and Pt are extensively studied because of their outstanding performance in the oxygen evolution reaction (OER) and hydrogen evolution reaction (HER) related to water splitting. Precious metal oxides play a vital role in improving the efficiency of water splitting, Both RuO_2 and IrO_2 are widely accepted as benchmark electrocatalysts for the oxygen evolution reaction, owing to their high electrocatalytic activities in both acidic and alkaline solutions. [37,38]

Experimental evidence shows that Ir and Ru materials exhibit high activity towards OER due to their superior stability, low Tafel value, and small overpotential when compared to Pt and Pd (Pt < Pd < Ir < Ru). [19, 39]

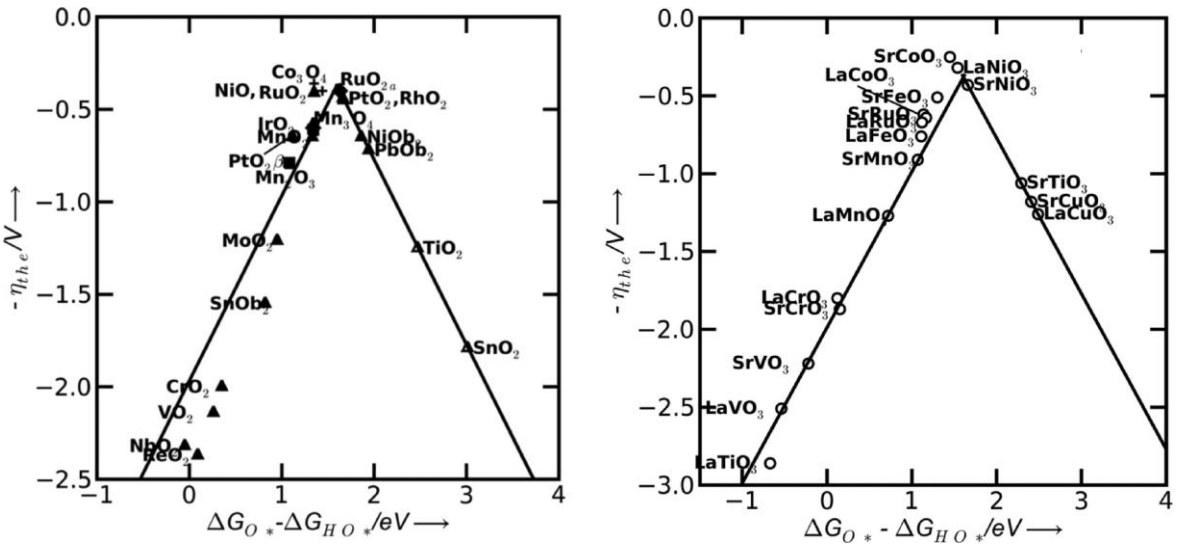

Figure 1.9: Theoretical overpotential for oxygen evolution *vs.* the difference between the standard free energy of two subsequent intermediates ($\Delta G^0_{O*} - \Delta G^0_{HO}$) for various binary oxides (left) and perovskite oxide (right). [40]

While not an oxide, Pt stands out as the most efficient catalyst for the hydrogen evolution reaction. This material exhibits outstanding catalytic performance and is frequently utilized as a benchmark in electrocatalytic research. RuO_2 exhibits the most excellent OER activity compared to other OER catalyst materials. Nonetheless, it is susceptible to significant corrosion when operating in acidic electrolytes. In the course of the OER process, it has been reported that oxygen molecules are generated from the lattice oxygen of RuO_2, leading to increased instability and significant depletion of the Ru element in the acidic electrolyte. [41, 42] To improve the stability of RuO_2, a doped bimetallic oxide system $Ru_xIr_{1-x}O_2$ was proposed. [43] Ir is a precious metal which is ten times scarcer than Pt. The limited availability and high cost of Ir restrict its widespread application as a catalyst. The OER activity of IrO_2 is marginally less than that of RuO_2 in acidic conditions, yet the durability of IrO_2 surpasses that of RuO_2 by a factor of twenty. [44]

An effective approach to enhance the stability of RuO_2 is to mix it with other metals (i.e., Pt [45]) and metal oxides (Ta_2O_5, [46] TiO_2, [47] SnO_2, [48] ZrO_2, [49] and Sb_2O_5[50]) to form mixed oxides. However, the high cost and limited accessibility of these noble-metal based oxides continue in obstructing their extensive commercialization. To tackle the issue of cost, it is crucial to investigate non-noble metal catalysts as HER and OER catalysts for water electrolysis.

1.1.4 Non-Noble-Metals Based Catalysts for HER and OER

Extensive research has been conducted for the development of efficient noble metal-free electrocatalysts for HER and OER, e.g., transition-metal (e.g., Mn, Fe, Co, and Ni) oxides, metals/alloys, [51] metal phosphides, carbides, nitrides, [52-56] single atoms, [57] functional carbon materials, [58] and various synergistic hybrids. [59, 60] These materials have been extensively studied and show high potential for use in the HER and OER. [61]

As a large category of inorganic solids, metal oxides composed of low-cost and earth-abundant elements have been an important family of functional materials. In comparison to other types of metal compounds, a clear superiority of metal oxides lies in the compositional and structural diversity, which provides an electronic and crystal structure flexibility. The advantages of compositional and structural diversity, along with flexible tunability, ease of synthesis and environmental friendliness, have led to significant interest in metal oxide-based materials for electrocatalysis applications. [30, 62-66]

Recent developments in metal oxide-based HER and OER electrocatalysts includes single transition metal oxides, perovskites, spinels, metal (oxy)hydroxides, and oxide-containing hybrids that have been employed for efficient electrocatalysis.

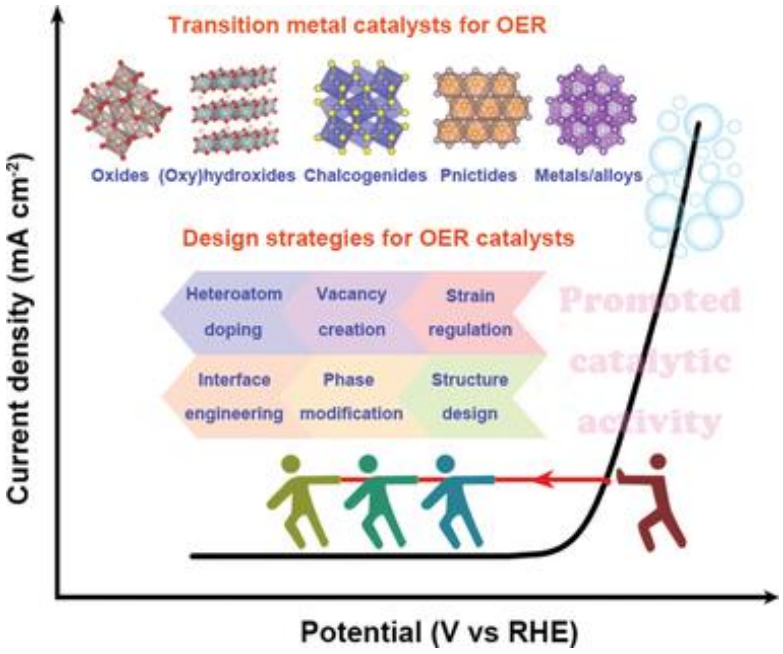

Figure 1.10: Schematic illustration of transition metal-based electrocatalysts for OER and the potential strategies for performance enhancement. [67]

1.2 Transition Metal Oxides

For the past three decades, various metal oxides have been studied for electrochemical water splitting approaches. The focused aim in the field of clean energy production and storage is to fabricate non-precious, highly active and stable catalysts. Several earth abundant metal oxides such as Co_3O_4, [68] Mn_3O_4, [69] MoO_3 [70] and NiO [71] have been attempted for electrochemical water splitting due to their suitable physico-chemical properties and earth abundance. Metal oxides typically exhibit high electrochemical stability over extended periods and demonstrate significant stability in alkaline electrolyte mediums when compared to other metal derivatives, including metal chalcogenides, phosphates, carbides, and nitrides etc. [72] They are regarded as outstanding catalysts for both OER and HER activities. However, there are certain drawbacks linked to single metal oxides. In the context of electrochemical water oxidation, poor electrical conductivity, electrochemical response and slow reaction kinetics are the major problems encountered by the researchers during the reaction. [73]

Therefore, exploring new kinds of transition metal oxides (TMOs) and devise efficient strategies (**Figure 1.11)** to further enhance their OER activities is required.

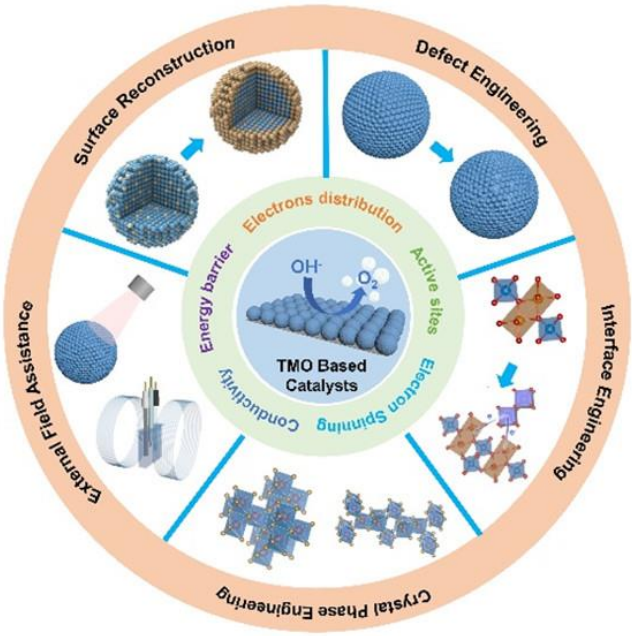

Figure 1.11: Regulation strategies of metal oxide-based electrocatalyst. [74]

The regulation strategies used for enhancing the OER activities of TMO-based electrocatalysts encompass electronic structure modulation through defect engineering, through doping, surface reconstruction, phase engineering, interface engineering and the application of an external field. [74]

1.2.1 REGULATION STRATEGIES

1.2.1.1 Defects Engineering

Usually, defects (anion defects or cation defects) engineering can significantly alter the catalytic properties of TMO-based electrocatalysts by influencing their localized electronic structure and orbital distributions.

1.2.1.2 Anion Defects

In TMO-based electrocatalysts, anion vacancy typically indicates the presence of oxygen vacancies (V_O). V_O can tune the electronic structure of electrocatalysts by decreasing the coordination members of metal sites to promote the adsorption of intermediates on the catalysts and subsequently improving the reaction thermodynamics and kinetics, a recent report is V_O-CoO. [75] The introduction of V_O enables the hybridization of O 2*p*, Co 3*d* and Co 3*s* in the bandgap to generate new electronic states that promotes enhanced charge transfer for the OER. A recent study examined $NdNiO_3$ (NNO) with varying V_O concentrations and systematically investigated the correlation between V_O and OER performance. The optimal OER activity was attained when the V_O concentration and the Ni^{3+} /Ni^{2+} ratio was balanced to ensure a moderate binding energy with *OH and a more favourable occupancy of the e_g orbital. [76]

1.2.1.3 Cation Defects

Metal vacancies are more stable than oxygen vacancies (V_O) and can facilitate electron delocalization while offering active sites. More attention has been paid to the control cation defects in TMO. [76] Wang *et al*. investigated the influence of Sn vacancies in $SnCo_{0.9}Fe_{0.1}(OH)_6$ by Ar plasma treatment. [77] The as-formed Sn vacancies result in an amorphous surface and exposed more active CoFe sites and reduce their coordination number, thereby optimizing the adsorption energy of O* on Co sites. Defects usually serve as the final active sites for the OER process. [77]

1.2.1.4 Doping Effects

The geometry and electronic structure serve as crucial parameters for optimization in the development of efficient HER and OER catalysts, alongside considerations of electrocatalyst type and chemical stability. [78] Doping serves as a prevalent and effective method for tailoring the electronic structure of catalytic materials. Adjusting the electronic

structure is a critical factor of enhancing OER activities, and elemental doping is one of the best ways of tuning the electronic structure. [79] The tuning of the electronic structure through doping affects the binding energy of OER intermediates, including *O, *OH and *O–OH. Therefore, in comparison to other approaches for enhancing OER activities, doping presents a viable solution for attaining significant activity and enduring stability even under extreme anodic overpotentials.

The enhancement of the Oxygen Evolution Reaction (OER) in perovskite oxides can be achieved using various doping strategies that alter their electronic structure and catalytic characteristics.

Substituting A-site or B-site cations in the perovskite structure through cation doping is a method aimed at improving HER and OER activity. The enhancement of activity and durability in $SrRuO_3$ perovskite is primarily achieved through the doping of the Sr site with Na ($Sr_{0.95}Na_{0.05}RuO_3$), leading to a decrease in octahedral distortion and an increase in the oxidation state. [80] For example, the co-doping of transition metals like iron (Fe) and tin (Sn) has demonstrated the ability to stabilize a cubic perovskite structure, leading to a notable enhancement in OER performance. The ideal formulation of $BaCo_{0.9-x}Fe_xSn_{0.1}O_{3-\delta}$ (x = 0.2) exhibited an inherent OER performance surpassing that of IrO_2 in alkaline environments. [81] The doping of $SrTiO_3$ at the B-site with cobalt and iron elements ($SrCo_{0.9}Ti_{0.1}O_{3-\delta}$) exhibited enhanced OER activity due to its optimized e_g filling value, leading to an improved electrocatalyst for the OER. [82]

1.2.2 ABO_3-type Perovskites and Ilmenite Structures

ABO_3-type represents two unique and important crystallographic structures in the field of materials science, especially regarding catalysis and electronic characteristics. The ABO_3-type ilmenite exhibits an ordered corundum structure, characterized by layers of AO_6 octahedra

that are sandwiched with two layers of BO_6 octahedra, representing a modified α-Al_2O_3 structure, as illustrated in **Figure.1.12**. [83]

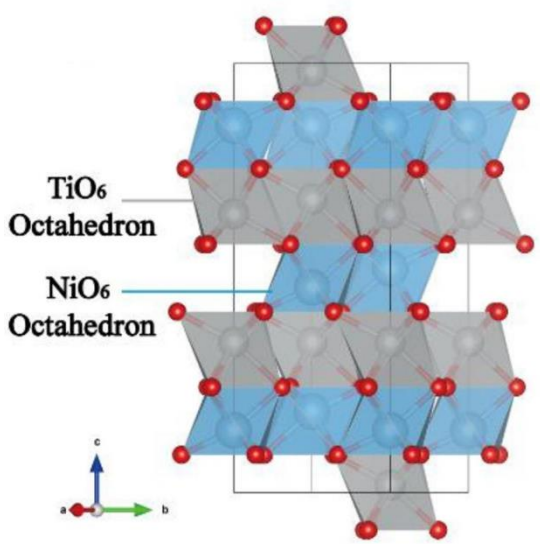

Figure 1.12: Lattice diagram of ilmenite $NiTiO_3$. [84]

Metal titanates ($ATiO_3$), where A = Pb, Mn, Fe, Co, Ni, Cu, or Zn, are recognized as inorganic functional materials with wide uses. The compounds exhibiting an ilmenite structure within the trigonal system hold significant relevance as chemical and electrical materials, attributed to their weak magnetism and semiconductivity. [85]

In the early 1920s, Goldschmidt proposed a "tolerance factor" (*t*) to analyze the stability of perovskites. The tolerance factor *t* proposed by Goldschmidt has gained significant acceptance as a key criterion for the formation of the perovskite structure.

The criterion of ABO_3-type ilmenite formability is expressed by the following equations:

$$t = \frac{1}{3}\left(\frac{(\sqrt{2}+1)R_O^{-2}+R_B)}{R_O^{-2}+R_A} + \frac{\sqrt{2}R_O^{-2}}{R_O^{-2}+R_B}\right) \quad (1.12)$$

Where R_A, R_B and R_O are the ionic radii of A, B and O respectively and should be between $1 > t > 0.745$. Another necessary condition is electronegativity difference (abbreviated to e) of the present ABO_3-type ilmenite $e > 1.465$. [83, 86]

Recently, Barman *et al*. [87] reported the catalytic performance of ilmenite $NiTiO_3$ nanoparticles for the oxygen evolution reaction, in terms of durability and efficiency, perovskite-type $NiTiO_3$ materials have demonstrated exceptional stability throughout the cycling process. Guiet *et al*. reported that $Ni_{0.8}Cu_{0.2}TiO_3$ nano oxide is highly active and stable material for O_2 evolution. [88]

The stability and good electrocatalytic activity of ilmenite-based compounds necessitate further exploration to develop efficient OER catalysts.

1.2.3 Perovskites Oxide

Perovskite oxides represent a diverse group of functional metal oxides characterized by the general formula ABO_3. In this structure, the larger A-site cations are typically rare-earth or alkaline earth metals, while the smaller B-site cations are often transition metals, exhibiting 12-fold and 6-fold oxygen coordination, (**Figure 1.13**) respectively. This leads in a vast array of oxides with a wide range of properties. In the 1990s, A-site deficient $Sr_{1-x}NbO_{3-\delta}$ was reported for catalyzing HER in strong acids; however, the HER activity was notably low. [89, 90] Significant efforts have been dedicated to enhancing the HER catalytic performance of perovskite oxides through a multi-strategy design, resulting in significant advances. The HER electrocatalysts based on three types of perovskite oxides (i.e., simple perovskites, double perovskites and Ruddlesden–Popper-type oxides) are developed.

1.2.3.1 Simple Perovskites

A pioneering investigation conducted by Xu *et al*. reported an A-site praseodymium (Pr)-doped $Pr_{0.5}(Ba_{0.5}Sr_{0.5})_{0.5}Co_{0.8}Fe_{0.2}O_{3-\delta}$ (Pr0.5BSCF) perovskite characterized by a cubic structure, demonstrating its efficacy and stability as an electrocatalyst for HER in alkaline environment. [91] Pr0.5BSCF shows a significant enhancement of HER catalytic activity as compared to the undoped $Ba_{0.5}Sr_{0.5}Co_{0.8}Fe_{0.2}O_{3-\delta}$ (BSCF) perovskite which is ascribed to the

Pr-doping induced changes in surface electronic structures and properties. Zhu *et al*., and group prepared $SrNb_{0.1}Co_{0.7}Fe_{0.2}O_{3-\delta}$ perovskite nanorod (SNCF-NR), $La_{0.5}(Ba_{0.4}Sr_{0.4}Ca_{0.2})_{0.5}Co_{0.8}Fe_{0.2}O_{3-\delta}$ (LBSCCF) by a facile electrospinning method, displaying excellent HER activity and stability in the basic electrolyte. [92, 93]

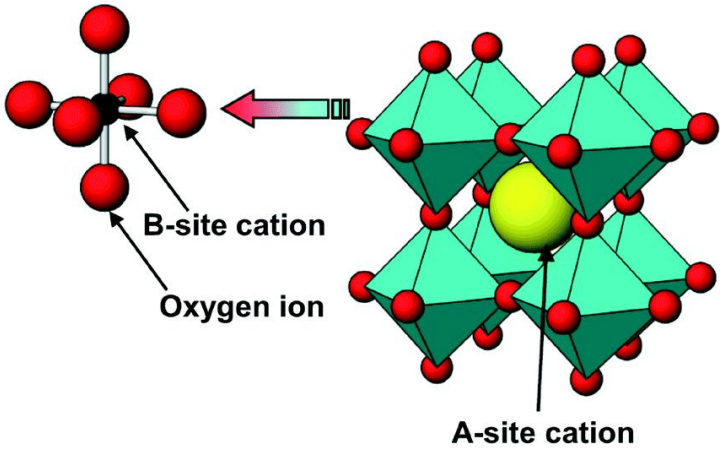

Figure 1.13: Sketch of a basic ABO_3 perovskite oxide structure. [94]

1.2.3.2 Double Perovskites

Double perovskite oxides with a formula of $AA'B_2O_{5+\delta}$ have a layered structure with alternating layers of $|AO_\delta|BO_2|A'O|BO_2$, where generally A is a large-radii alkaline-earth metal element (e.g., Ba), A' is a small-radii lanthanide element (e.g., La, Pr, Nd, Gd), B is transition metal element, and the oxygen vacancies are located in the AO layer. Double perovskites feature some unique electronic structures that are typically not found in single perovskites, [95, 96] which may generate several benefits to the HER electrocatalysis. Guan *et al*. carried out a systematic study on A-site ordered $RBaCo_2O_{5.5+\delta}$ (R = lanthanides) double perovskites for alkaline HER electrocatalysis. [97] It was proposed that the A-site ionic electronegativity (AIE) could act as a valuable unifying descriptor for predicting the HER activities of 13 cobalt-based perovskites. The compound $(Gd_{0.5}La_{0.5})BaCo_2O_{5.5+\delta}$, with an AIE value of approximately 2.33, demonstrated the highest activity. (**Figure 1.14**). [98] The peak HER activity at a moderate

AIE value of ~2.33 can be associated with the optimal electronic states of active B-sites via an inductive effect in perovskite structure (**Figure. 1.15**).

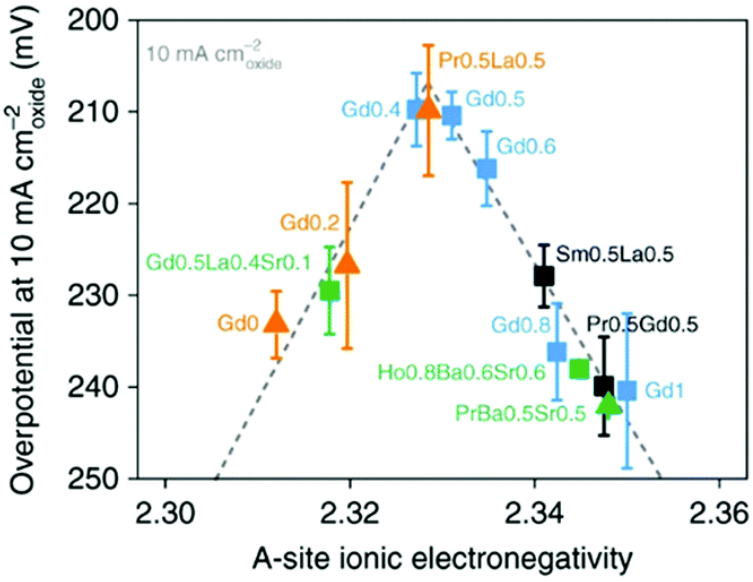

Figure 1.14: HER activity trends of overpotential at 10 mAcm^{-2} oxide as a function of A-site ionic electronegativity. [98]

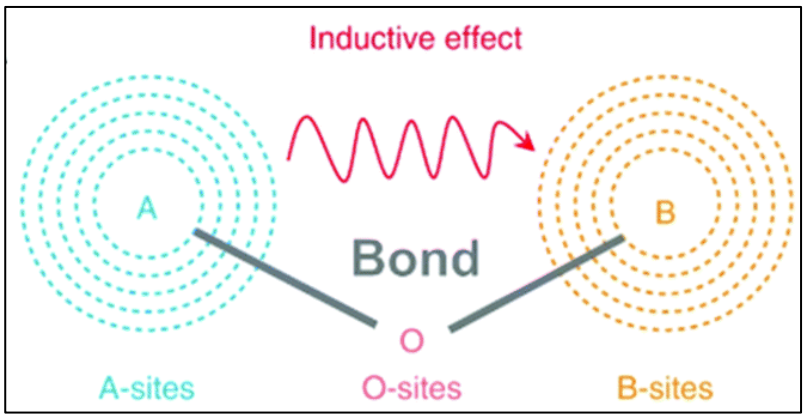

Figure 1.15: Inductive effects and electron exchange interactions between A-sites and B-sites in perovskites from molecular orbital theory. [98]

1.2.3.3 Ruddlesden–Popper-type Oxides

Layered Ruddlesden Popper (RP) type oxides (formula of $A_{n+1}B_nO_{3n+1}$ or equivalently $AO(ABO_3)_n$, wherein n ABO_3 perovskite layers are sandwiched between two AO rock-salt layers (**Figure 1.16)**, have received considerable attention due to their chemical flexibility, layered structure, wide element accommodation and labile lattice. [99, 100] Sr_2RuO_4 oxide presents an ultrahigh HER activity in alkaline media. This work emphasizes the advantages of RP-layered oxides can benefit from their unique structural features and thus boost the alkaline

HER through combined control over key HER steps such as water dissociation and hydrogen adsorption**.** [101] We note that the utilization of RP-layered oxides as the HER electrocatalysts is currently in its early stages. One direction of future research is to develop RP-type oxides composed of nonprecious transition metals such as Fe, Co and Ni as potential catalysts for the HER, since Ru is a costly metal that can impose restrictions on practical applications. [102]

One direction of future research is to develop RP-type oxides composed of non-noble transition metals as potential catalysts for the HER.

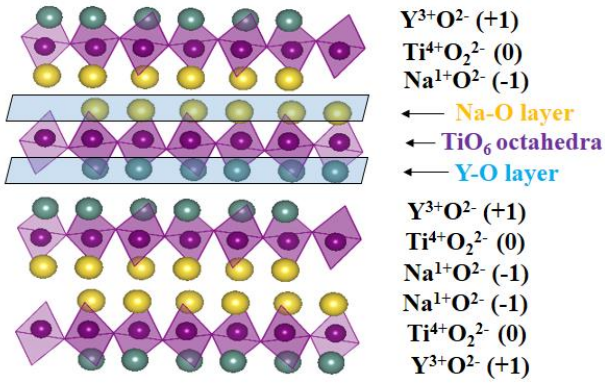

Figure 1.16: Sketch of $NaYTiO_4$ Ruddlesden–Popper-type oxide structure plotted from VESTA software.

1.3 Key Performance Evaluating Parameters for HER and OER

1.3.1 Overpotential (η)

The overpotential at a defined current density (typically 10 mA cm^{-2}) serves as a crucial activity parameter, frequently employed as the main assessment criterion for electrocatalytic activity in both HER and OER electrocatalysts in all media. The overpotential of an electrochemical process refers to the additional potential required to sustainably drive a reaction from its reversible voltage. [103, 104] The reversible potentials for HER and OER are 0 V and 1.23 V *vs.* the reversible hydrogen electrode (RHE), respectively. Therefore, the equations for the OER and the HER are given by $\eta_{OER} = E_{RHE} - 1.23\,V$ and $\eta_{HER} =$

$E_{RHE} - 0\,V$, respectively. The current density of 10 $mAcm^{-2}$ serves as a standard for evaluating the performance of electrocatalytic materials in the context of HER and OER across all mediums. [105]

In electrochemical reactions, various sources of overpotential exist, the overpotential arising from the intrinsic resistance of the catalysts, known as charge transfer resistance (R_{ct}), the overpotential related to solution resistance (R_s) or uncompensated resistance (R_u), and the overpotential caused by the concentration difference ($\eta_{conc.}$) of electroactive species at the electrocatalytic surface compared to the bulk.

The overpotential resulting from the intrinsic resistance (R*ct*) of the electrocatalyst can be minimized by adjusting the electronic properties of the materials at the nanoscale or by combining them with synergistic support materials such as graphene, CNTs, carbon dots, and others, both at the catalytic surface and in bulk. [106]

The overpotential resulting from uncompensated or solution resistance cannot be significantly minimized, as it is minimally affected by the electrode fabrication method and the characteristics of the catalytically active interface. The uncompensated or solution resistance represents the total of the resistances generated at different junctions within the circuit, including the connecting points and the distance between the reference electrode and the working electrode. This can be significantly reduced by designing the electrochemical cell in such a way that the distance between the reference, counter, and working electrodes are minimum.

The overpotential arising from the concentration gradient of electroactive species at catalytic sites compared to the bulk can be mitigated through the agitation of the electrolyte using mechanical stirring or sonication. [104]

1.3.2 Tafel Slope

Tafel analysis serves as an important study for evaluating electrocatalysts employed in water electrolysis. Through the analysis of the Tafel slopes for both the oxygen evolution reaction and the hydrogen evolution reaction, we obtain valuable insights into the fundamental kinetics of the electrocatalyst being studied. This analysis facilitates predicting the kinetics associated with electrocatalytic reactions taking place at the catalytic interface. The Tafel slope is often linked to the mechanism of the hydrogen evolution reaction at a specific electrocatalytic interface. A notably low Tafel slope, generally ranging from 30 to 40 mV dec^{-1}, indicates that the hydrogen evolution reaction proceeds through a more rapid and efficient Tafel pathway. [103] The Volmer–Heyrovsky mechanism stands out as the primary pathway identified in numerous non-precious metal-based electrocatalysts for hydrogen evolution reactions, including chalcogenides of Fe, Co, Ni, W, and Mo. The Tafel slope noted in this mechanism generally falls between 50 and 120 mV dec^{-1}, influenced by the availability of surface-active sites essential for the reaction. It is important to highlight that these mechanisms are predominantly relevant in acidic environments. Nonetheless, predicting the mechanism of OER through the Tafel slope presents more complexity compared to HER, primarily because of the multiple intermediate steps involved in the anodic half-cell reaction of water electrolysis. [107]

The Tafel slope measurements are used to assess the intrinsic electron transport at the electrode/electrolyte interface. From the derived Butler-Volmer equation at both higher anodic and cathodic overpotentials, it follows the Tafel equation, indicating that the current density j is directly proportional to the exchange current density j_0 and inversely proportional to the Tafel slope b. It is given as,

$$j = j_0 \log(\eta/\mathrm{b}) \tag{1.13}$$

where, j is the current density, j_0 is the exchange current density, η is the overpotential and b is the Tafel constant. [108, 109] Typically, the Tafel plot is derived by transforming the polarization curve, such as the linear sweep voltammogram (LSV), into a graph of log(j) against η. The slope of the linear segment on the Tafel plot represents the relationship between the overpotential and the current density. which is expressed as follows:

$$\log(j)/\mathrm{d}\eta = 2.303\mathrm{RT}/\alpha\mathrm{nF} \quad (1.14)$$

The Tafel slope is inversely proportional to the charge transfer coefficient (α), as the remaining other parameters are constants (viz., the ideal gas constant (R), temperature (T), Faraday constant (F), and the number of electrons transferred (n), which is equal to 4 for the OER and 2 for the HER). This suggests that a catalyst exhibiting a high charge transfer ability is expected to have a low Tafel slope. This is why it is frequently utilized as a key activity parameter in assessing catalytic activity. The LSV acquired at the lowest possible scan rate provides the Tafel slope with minimal inaccuracy. [110] However, as it is potentiodynamic, the observed current cannot be the actual one and leading to potential discrepancies that could affect the Tafel slope values. Therefore, the potentiostatic analysis is essential for achieving a steady state current, and based on this, the static current densities observed at various overpotentials can be utilized to derive Tafel slope values, offering greater accuracy in comparison to the potentiodynamic method. Furthermore, electrochemical techniques such as chronoamperometry, chronopotentiometry, and electrochemical impedance spectroscopy (EIS) provide alternative approaches for analysing Tafel plots with better accuracy.

1.3.3 Electrochemically Accessible/Active Surface Area (ECSA)

The ECSA indicates the intrinsic catalytic characteristics of the catalyst being studied in the context of water electrolysis. The double layer capacitance (C_{dl}) serves as a quantitative measure of the surface area accessible to the electrolyte ions. [111] The electrochemical

double-layer capacitance of the catalytic surface can be used to estimate ECSA. [112] There are two distinct methods to determine the electrochemical capacitance: (1) through the assessment of the non-Faradaic capacitive current associated with double-layer charging, derived from the scan-rate dependence cyclic voltammograms (CVs) and (2) by evaluating the frequency-dependent impedance of the system using electrochemical impedance spectroscopy (EIS). [113] To assess double-layer charging through cyclic voltammetry, a non-Faradaic potential range of approximately 0.1 V can be determined from static cyclic voltammetry analysis. It is assumed that all measured current in this non-Faradaic potential region arises from double-layer charging. The double-layer charging current is determined by multiplying the scan rate ν by the electrochemical double-layer capacitance C_{dl}, as given by equation 1.14. [114]

$$i_c = \nu C_{dl} \tag{1.15}$$

Thus, a plot of i_c as a function of ν yields a straight line with a slope equal to C_{dl}.

The ECSA of a catalyst sample is calculated from the double layer capacitance according to equation:

$$ECSA = C_{dl}/C_s \tag{1.16}$$

where C_s is the specific capacitance of the sample or the capacitance of an atomically smooth planar surface of the material per unit area under identical electrolyte conditions. [115]

1.3.4 Turnover Frequency (TOF)

The TOF is used as a quantitative metric for assessing an electrocatalyst at a defined overpotential. The turnover frequency of the catalyst is characterized by the number of moles of O_2/H_2 evolved per unit time. Since both HER and OER exhibit pseudo first order

kinetics, their TOF are expressed per unit time. The equation presented here is used to determine the TOF for an electrocatalytic gas evolution reaction:

$$\text{TOF} = jN_A/nAF\Gamma \quad (1.17)$$

where j is the current density (A cm^{-2}), N_A is the Avogadro constant, A is the geometrical surface area, n is the number of electrons transferred to evolve a molecule of product (for H_2, it is 2 and for O_2, it is 4) and Γ is the surface or total concentration of catalyst in terms of number of atoms. The TOF presents an additional kinetic parameter for various electrocatalysts; however, its application is limited due to challenges in determining the surface concentration or the active sites on the surface. The strong dependency of the active surface concentration on the determination method presents a limitation, making TOF less effective as a primary activity parameter for assessing materials in water splitting electrocatalysis. [116]

Several methods are available for determining the surface or total concentration of a catalyst in terms of number of atoms. The redox peak observed in the cyclic voltammogram serves as a means to determine the surface concentration following the catalyst's activation through CV cycling. [117] The total atom concentration can also be derived using Avogadro's number in conjunction with the average particle diameter of the catalyst. Additionally, one can employ the assumption of a monolayer as another approach. [118]

1.3.5 Faradaic Efficiency (FE)

Faradaic efficiency serves as a quantitative measure for both the HER and OER, as it is intrinsically linked to the efficiency of electrolysis. The efficiency of an electrocatalyst can be characterized by its ability to transfer electrons supplied by the external circuit across the interface to the electroactive species, thereby influencing the electrode reaction, whether it be the hydrogen evolution reaction or the oxygen evolution reaction. [119]

The two most widely accepted methods include the electrochemical approach, which employs the rotating ring disk electrode (RRDE) experiment, specifically applicable to the OER. [120, 121]

Following is the equation used for the calculation of Faradaic efficiency by RRDE method**:** [120]

$$FE = I_R \times n_D / I_D \times n_R \times N_{CL} \quad (1.18)$$

where I_R and I_D are the current at the ring and disc, respectively, n_R and n_D are the numbers of electrons transferred at the ring and disc, respectively, and N_{CL} is the collection efficiency of the RRDE used.

The second approach to assessing Faradaic efficiency is applicable to both the HER and OER. The amount of gas (H_2/O_2) evolved is determined through integration derived from the chronoamperometric or chronopotentiometric analysis. The quantity of gas (H_2/O_2) practically obtained is then calculated, which can be done by conventional water gas displacement method and the gas chromatography. [119]

1.3.6 Mass Activity and Specific Activities

The activity of electrocatalysts is certainly affected by the catalyst loading, making it crucial to correlate the measured current densities with this parameter for the accurate calculation of mass activity. The concept of "mass activity" denotes the current normalized against the loaded mass of a catalyst, usually expressed in Ag^{-1}. [122] On the other hand, the current density normalized by the geometrical area of the electrode, typically represented in mA cm^{-2}, effectively represents the actual area of electrodes that possess smooth and planar surfaces. In the context of roughened electrocatalytic surfaces, commonly examined in the studies of hydrogen evolution reaction and oxygen evolution reaction, mass-normalized activity is more

suitable, resulting in less biased outcomes. A model catalyst surface (**Figure 1.17)** that illustrates the concepts of geometric activity, specific activity and mass activity.

Thus, employing mass-normalized activity alongside geometrical area-normalized activity offers a more thorough insight into the catalytic characteristics, particularly for nonplanar and roughened interfaces like in situ grown catalysts.

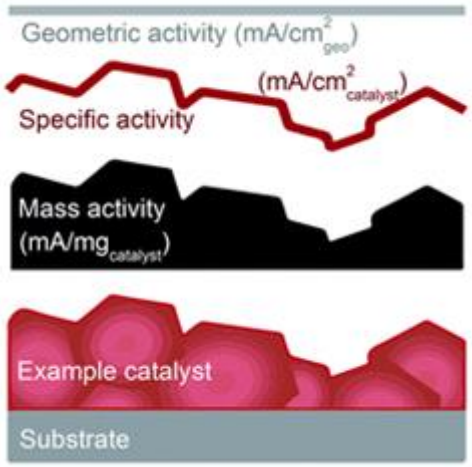

Figure 1.17: A model catalyst surface that visualizes the definition of geometric activity, specific activity and mass activity [123]

The current normalized by the electrochemical surface area (ECSA) or the Brunauer-Emmett-Teller (BET) surface area is referred to as specific activity and is expressed as A cm^{-2}. The BET surface area identified through gas adsorption and desorption represents the actual surface area of the catalyst, which does not necessarily have to be electrocatalytically active. The ECSA (or roughness factor)-normalized current density is preferable, as it demonstrates greater sensitivity to catalyst loading and will vary accordingly.

The current normalized by the ECSA (in units of A/cm^2_{ECSA}) accurately represents the intrinsic catalytic property of the catalyst, in contrast to the normalization based on the geometrical surface area. [124]

1.3.7 Screening an Electrocatalyst for Stability:

The stability of an electrocatalyst is crucial, as robustness is essential for practical and commercial applications. An efficient electrocatalyst is one that can sustain its stability,

activity, and morphology, remaining unaffected during corrosive electrocatalytic reaction conditions. In addition to the activity parameters concerning the kinetics and thermodynamics of HER and OER catalysis, the stability of an electrocatalyst is another crucial metric to be proven. It can be verified via both potentiostatic analyses like chronoamperometry (potential is static and current is monitored as a function of time) and chronopotentiometry (current is static and potential is monitored as a function of time) and potentiodynamic analysis like cyclic voltammetry at high scan rates usually ranges from 100 mV s^{-1} to 300 mV s^{-1} for 1000 to 5000 cycles. The negligible difference in activities before and after the stability studies ensures the stable nature of electrocatalyst. [125]

Recent findings demonstrated the stable characteristics of catalysts based on 3d-transition metals in alkaline OER and HER. Currently, the search for bi-functional catalysts is ongoing, aimed at substituting scarce metals while enhancing both activity and stability. The evaluation and critical consideration of parameters such as overpotential, Tafel slope, mass activity, TOF and stability are essential for the development of improved catalysts for electrocatalytic water splitting in multiple pH conditions.

The stability claims of a water splitting catalyst must be supported by a series of post-electrochemical characterizations to assess the structural and compositional stability of the catalyst. This includes techniques such as ex-situ and in-situ XRD, XPS, SEM, and TEM, in addition to potentiometric studies. [126-128]

1.4 Motivation and Objective of this Work

The electrolysis of water, which produces hydrogen and oxygen, has been the subject of research since long time. However, it continues to face challenges in terms of commercialization due to its overall low efficiency. For an effective electrocatalyst cost and stability are the primary requirements, together with superior catalytic activity, in this context, transition metal oxides are optimal choice due to their high stability, multi-valent states, ease of synthesis, tunable morphology, environmentally safe and economic abundance. Till date, various metal oxides based electrocatalysts have been reported for generation of oxygen and hydrogen. However, the challenge persists in overcoming the thermodynamic barrier more effectively, aiming for an overall efficiency of unity. This led to investigation into more suitable electrocatalytic materials to improve the overall efficiency of water splitting.

The primary aims of the present thesis work are as follows:

1) Selection of transition metal- based oxides due to their high stability and bulk conductivity for application as electrocatalytic materials.
2) Tuning of the redox energy level of transition metal (3*d*) with respect to O (2*p*) orbital in different lattices to develop efficient HER and OER catalyst
3) Understanding of the band -position conduction band (CB) and valence band (VB) of different transition metal ions to get HER
4) Doping of foreign elements into the lattice of semiconductor to study the effect on band position or redox level of O (2*p*)
5) Study of effect of electronegativity/ inductive effect of dopants in different lattices on electrocatalytic activity
6) Investigating the influence of defects in the lattice of transition metal oxides on their electrocatalytic performance

1.5 References

1. Lewis, N.S.; Nocera, D.G. Powering the planet: Chemical challenges in solar energy utilization. *Proceedings of the National Academy of Sciences.* **2006**, *103*, 15729–15735.
2. Global energy trends: Insights from the 2023 statistical review of world energy.
3. Yoro, K.O.; Daramola, M.O. CO_2 emission sources, greenhouse gases, and the global warming effect. *Elsevier eBooks.* **2020**, 3–28.
4. Owusu, P.A.; Asumadu-Sarkodie, S. A review of renewable energy sources, sustainability issues and climate change mitigation. *Cogent Eng.* **2016**, *3*, 1167990.
5. None, N. A national vision of America's transition to a hydrogen economy. To 2030 and beyond. *EERE Publication and Product Library, Washington, DC (United States)* **2002**.
6. Zhu, J.; Hu, L.; Zhao, P.; Lee, L.Y.S; Wong, K.Y. Recent advances in electrocatalytic hydrogen evolution using nanoparticles. *Chem. Rev.* **2016**, *120*, 851–918.
7. Balat, M. Potential importance of hydrogen as a future solution to environmental and transportation problems. *Int. J. Hydrogen Energy* **2008**, 33, 4013–4029.
8. Pilavachi, P.A.; Chatzipanagi, A.I.; Spyropoulou, A.I. Evaluation of hydrogen production methods using the Analytic Hierarchy Process. *Int. J. Hydrogen Energy* **2009**, *34*, 5294–5303.
9. Brar, S.K.; Permaul, K.; Pakshirajan, K.; de Carvalho, J.C. eds. *Biohydrogen-Advances and Processes*. Springer Nature Switzerland, Imprint: Springer. **2024**
10. Santos, D.M.F.; Sequeira, C. a. C.; Figueiredo, J.L. Hydrogen production by alkaline water electrolysis. *Química Nova* **2013**, *36*, 1176–1193.
11. Wang, M.; Wang, Z.; Gong, X.; Guo, Z. The intensification technologies to water electrolysis for hydrogen production – A review. *Renew. Sustain. Energy Rev*. **2013**, *29*, 573–588.
12. Zhang, H.; Maijenburg, A.W.; Li, X.; Schweizer, S.L.; Wehrspohn, R.B. Bifunctional heterostructured transition metal phosphides for efficient electrochemical water splitting. *Adv. Funct. Mater.* **2020**, *30*, 2003261.
13. Wang, J.; Yue, X.; Yang, Y.; Sirisomboonchai, S.; Wang, P.; Ma, X.; Abudula, A.; Guan, G. Earth-abundant transition-metal-based bifunctional catalysts for overall electrochemical water splitting: A review. *J. Alloys. Compd.* **2020**, *819*, 153346.
14. Yan, Y.; Xia, B.Y.; Zhao, B.; Wang, X. A review on noble-metal-free bifunctional heterogeneous catalysts for overall electrochemical water splitting. *J. Mater. Chem. A.* **2016**, *4*, 17587–17603.
15. Zou, X.; Zhang, Y. Noble metal-free hydrogen evolution catalysts for water splitting. *Chem. Soc. Rev.* **2015**, *44*, 5148–5180.
16. Grewe, T.; Deng, X.; Weidenthaler, C.; Schüth, F.; Tüysüz, H. Design of ordered mesoporous composite materials and their electrocatalytic activities for water oxidation. *Chem. Mater.* **2013**, *25*, 4926–4935.

17. Yu, M.; Budiyanto, E.; Tüysüz, H. Principles of water electrolysis and recent progress in cobalt-, Nickel-, and Iron-Based oxides for the oxygen evolution reaction. *Angew. Chem. International Edition* **2021**, 61, 202103824

18. Wei, C.; Rao, R.R.; Peng, J.; Huang, B.; Stephens, I.E.; Risch, M.; Xu, Z.J.; Shao-Horn, Y. Recommended practices and benchmark activity for hydrogen and oxygen electrocatalysis in water splitting and fuel cells. *Adv. Mater.* **2019**, 3, 1806296

19. Reier, T.; Oezaslan, M.; Strasser, P. Electrocatalytic Oxygen Evolution Reaction (OER) on Ru, Ir, and Pt Catalysts: A Comparative study of nanoparticles and bulk materials. *ACS Cat.* **2012**, *2*, 1765–1772.

20. Li, X.; Hao, X.; Abudula, A.; Guan, G.; Nanostructured catalysts for electrochemical water splitting: current state and prospects. *J. Mater. Chem. A* **2016**, 4, 11973–12000.

21. You; B.; Liu; X.; Hu; G.; Gul; S.; Yano; J.; Jiang; D.E.; Sun; Y.; 2017. Universal surface engineering of transition metals for superior electrocatalytic hydrogen evolution in neutral water. *J. Am. Chem. Soc.* **2017**, 139, 12283–12290.

22. Yeo, B.S.; Bell, A.T. Enhanced activity of Gold-Supported cobalt oxide for the electrochemical evolution of oxygen. *J. Am. Chem. Soc.* **2011**, 133, 5587–5593.

23. Zhou, L.-J.; Zhou, L.J.; Huang, X.; Chen, H.; Jin, P.; Li, G.D.; Zou, X. A high surface area flower-like Ni–Fe layered double hydroxide for electrocatalytic water oxidation reaction. *Dalton Trans.* **2015**, 44, 11592–11600.

24. Xu, J.; Li, J.; Xiong, D.; Zhang, B.; Liu, Y.; Wu, K.H.; Amorim, I.; Li, W.; Liu, L. Trends in activity for the oxygen evolution reaction on transition metal (M = Fe, Co, Ni) phosphide pre-catalysts. *Chem. Sci.* **2018**, 9, 3470–3476.

25. Jin, S. Are metal chalcogenides, nitrides, and phosphides oxygen evolution catalysts or bifunctional catalysts? *ACS Energy Lett.* **2017**, 2, 1937–1938.

26. Li, X.; Hao, X.; Abudula, A.; Guan, G. Nanostructured catalysts for electrochemical water splitting: current state and prospects. *J. Mater. Chem. A* **2016**, 4, 11973–12000.

27. Zou, X.; Zhang, Y. Noble metal-free hydrogen evolution catalysts for water splitting. *Chem. Soc. Rev.* **2015**, 44, 5148–5180.

28. Ge, Z.; Fu, B.; Zhao, J.; Li, X.; Ma, B.; Chen, Y. A review of the electrocatalysts on hydrogen evolution reaction with an emphasis on Fe, Co and Ni-based phosphides. *J. Mater. Sci.* **2020**, 55, 14081–14104.

29. Guo, Y.; Park, T.; Yi, J.W.; Henzie, J.; Kim, J.; Wang, Z.; Jiang, B.; Bando, Y.; Sugahara, Y.; Tang, J.; Yamauchi, Y. Nanoarchitectonics for Transition-Metal-Sulfide-Based electrocatalysts for water splitting. *Adv. Mater.* **2019**, 31, 1807134.

30. Suen, N.-T.; Hung, S.F.; Quan, Q.; Zhang, N.; Xu, Y.J.; Chen, H.M. Electrocatalysis for the oxygen evolution reaction: recent development and future perspectives. *Chem. Soc. Rev.* **2017**, *46*, 337–365.

31. Ismail, N.; Qin, F.; Fang, C.; Liu, D.; Liu, B.; Liu, X.; Wu, Z.L.; Chen, Z.; Chen, W. Electrocatalytic acidic oxygen evolution reaction: From nanocrystals to single atoms. *Aggregate* **2021**, *2*, 106.

32. Lyons, M.E.G.; Burke, L.D. Mechanism of oxygen reactions at porous oxide electrodes. Part 1.-Oxygen evolution at RuO2 and RuxSn1–xO2 electrodes in alkaline solution under vigorous electrolysis conditions. *J. Chem. Soc., Faraday Trans. 1* **1987**, 83, 299-321.

33. Lyons, M.E.G.; Floquet, S. Mechanism of oxygen reactions at porous oxide electrodes. Part 2—Oxygen evolution at RuO_2, IrO_2 and $Ir_xRu_{1-x}O_2$ electrodes in aqueous acid and alkaline solution. *Phys. Chem. Chem. Phys.* **2011**, 13, 5314-5335.

34. Subbaraman, R.; Tripkovic, D.; Chang, K.C.; Strmcnik, D.; Paulikas, A.P.; Hirunsit, P.; Chan, M.; Greeley, J.; Stamenkovic, V.; Markovic, N.M. Trends in activity for the water electrolyser reactions on 3d M(Ni,Co,Fe,Mn) hydr(oxy)oxide catalysts. *Nat. Mater.* **2012** ,11, 550–557.

35. Subbaraman, R.; Tripkovic, D.; Strmcnik, D.; Chang, K.C.; Uchimura, M.; Paulikas, A.P.; Stamenkovic, V.; Markovic, N.M. Enhancing hydrogen evolution activity in water splitting by tailoring Li + -Ni(OH) 2 -PT interfaces. *Science* **2011,** 334, 1256–1260.

36. Stratton, S.M.; Zhang, S.; Montemore, M.M. Addressing complexity in catalyst design: From volcanos and scaling to more sophisticated design strategies. *Surf. Sci. Rep.* **2023**, *78* 100597.

37. Frydendal, R.; Paoli, E.A.; Knudsen, B.P.; Wickman, B.; Malacrida, P.; Stephens, I.E.; Chorkendorff, I. Benchmarking the stability of oxygen evolution Reaction catalysts: The importance of monitoring mass loss. *ChemElectroChem* **2014** ,1, 2075–2081.

38. Lee, Y.; Suntivich, J.; May, K.J.; Perry, E.E.; Shao-Horn, Y. Synthesis and activities of rutile IrO_2 and RuO_2 nanoparticles for oxygen evolution in acid and alkaline solutions. *J. Phys. Chem. Lett.* **2012**, 3, 399–404.

39. Jiao, Y.; Zheng, Y.; Jaroniec, M.; Qiao, S.Z. Design of electrocatalysts for oxygen- and hydrogen-involving energy conversion reactions. *Chem. Soc. Rev.* **2015**, *44*. 2060–2086.

40. Man, I.C.; Su, H.Y.; Calle-Vallejo, F.; Hansen, H.A.; Martínez, J.I.; Inoglu, N.G.; Kitchin, J.; Jaramillo, T.F.; Nørskov, J.K.; Rossmeisl, J. Universality in oxygen evolution electrocatalysis on oxide surfaces. *ChemCatChem* **2011**, *3*, 1159-1165.

41. Sun, H.; Jung, W. Recent advances in doped ruthenium oxides as high-efficiency electrocatalysts for the oxygen evolution reaction. *J. Mater. Chem. A* **2021**, *9*, 15506–15521.

42. Over, H. Fundamental studies of Planar Single-Crystalline Oxide model electrodes (RuO_2, IrO_2) for acidic water splitting. *ACS Catal.* **2021**, 11, 8848–8871.

43. Audichon, T.; Mamaca, N; Morais, C.; Servat, K.; Napporn, T.W.; Mayousse, E.; Guillet, N.; Kokoh, K.B. Synthesis of RUXIR1-XO2 anode electrocatalysts for proton exchange membrane water electrolysis. E*CS Trans.* **2013**, 45, 47.

44. Peng, Y.; Liao, Y.; Ye, D.; Meng, Z.; Wang, R.; Zhao, S.; Tian, T.; Tang, H. Recent advances regarding precious Metal-Based electrocatalysts for acidic water splitting. *Nanomaterials* **2022**, 12 2618.

45. Yao, W.; Yang, J.; Wang, J.; Nuli, Y. Chemical deposition of platinum nanoparticles on iridium oxide for oxygen electrode of unitized regenerative fuel cell. *Electrochem. Commun.* **2007**, 9 1029–1034.

46. Ardizzone, S.; Bianchi, C.L.; Cappelletti, G.; Ionita, M.; Minguzzi, A.; Rondinini, S.; Vertova, A. Composite ternary SnO2–IrO2–Ta2O5 oxide electrocatalysts. *J. Electroanal. Chem.* **2006**, 586, 160–166.

47. Da Silva, L.A.; Alves, V.A.; Da Silva, M.A.P.; Trasatti, S.; Boodts, J.F.C. Oxygen evolution in acid solution on IrO_2 + TiO_2 ceramic films. A study by impedance, voltammetry and SEM. *Electrochim. Acta* **1997**, 42, 271–281.

48. Balko, E.N.; Nguyen, P.H. Iridium-tin mixed oxide anode coatings. *J. Appl. Electrochem.* **1991**, 21, 678–682.

49. Benedetti, A.; Riello, P.; Battaglin, G.; De Battisti, A.; Barbieri, A. Physicochemical properties of thermally prepared Ti-supported IrO_2+ ZrO_2 electrocatalysts. *J. Electroanal. Chem.* **1994**, 376, 195–202.

50. Chen, G.; Chen, X.; Yue, P.L. Electrochemical behavior of novel Ti/IrO_X−Sb_2O_5−SnO_2 anodes. *J. Phys. Chem. B* **2002** ,106, 4364–4369.

51. Lu, Q.; Wang, A.L.; Gong, Y.; Hao, W.; Cheng, H.; Chen, J.; Li, B.; Yang, N.; Niu, W.; Wang, J.; Yu, Y. Crystal phase-based epitaxial growth of hybrid noble metal nanostructures on 4H/fcc Au nanowires. *Nat. Chem.* **2018**, 10, 456–461.

52. Chen, Z.; Duan, X.; Wei, W.; Wang, S.; Ni, B.J. Recent advances in transition metal-based electrocatalysts for alkaline hydrogen evolution. *J. Mater. Chem. A* **2019**, 7, 14971–15005.

53. Sun, H.; Yan, Z.; Liu, F.; Xu, W.; Cheng, F.; Chen, J. Self-Supported Transition-Metal-Based electrocatalysts for hydrogen and oxygen evolution. *Adv. Mater.* **2020**, 32, 1806326.

54. Zhu, Y.; Tahini, H.A.; Wang, Y.; Lin, Q.; Liang, Y.; Doherty, C.M.; Liu, Y.; Li, X.; Lu, J.; Smith, S.C.; Selomulya, C. Pyrite-type ruthenium disulfide with tunable disorder and defects enables ultra-efficient overall water splitting. *J. Mater. Chem. A* **2019**, 7, 14222–14232.

55. Hu, E.; Feng, Y.; Nai, J.; Zhao, D.; Hu, Y.; Lou, X.W.D. Construction of hierarchical Ni–Co–P hollow nanobricks with oriented nanosheets for efficient overall water splitting. *Energy Environ. Sci.* **2018**, 11, 872–880.

56. Zhou, H.; Yu, F.; Liu, Y.; Sun, J.; Zhu, Z.; He, R.; Bao, J.; Goddard, W.A.; Chen, S.; Ren, Z. Outstanding hydrogen evolution reaction catalyzed by porous nickel diselenide electrocatalysts. *Energy Environ. Sci.* **2017**, 10, 1487–1492.

57. Chen, Y.; Ji, S.; Chen, C.; Peng, Q.; Wang, D.; Li, Y. Single-Atom Catalysts: Synthetic strategies and electrochemical applications,' *Joule* **2018**, 2, 1242–1264.

58. Wang, J.; Xu, F.; Jin, H.; Chen, Y.; Wang, Y. Non-Noble Metal-based carbon Composites in Hydrogen Evolution Reaction: Fundamentals to Applications. *Adv. Mater.* **2017**, 29, 1605838.

59. Wang, H.; Fu, W.; Yang, X.; Huang, Z.; Li, J.; Zhang, H.; Wang, Y. Recent advancements in heterostructured interface engineering for hydrogen evolution reaction electrocatalysis. *J. Mater. Chem. A* **2020**, 8, 6926–6956.

60. Cobo, S.; Heidkamp, J.; Jacques, P.A.; Fize, J.; Fourmond, V.; Guetaz, L.; Jousselme, B.; Ivanova, V.; Dau, H.; Palacin, S.; Fontecave, M. A Janus cobalt-based catalytic material for electro-splitting of water. *Nat. Mater.* **2012**, 11, 802–807.

61. Zhu, Y.; Lin, Q.; Zhong, Y.; Tahini, H.A.; Shao, Z.; Wang, H. Metal oxide-based materials as an emerging family of hydrogen evolution electrocatalysts. *Energy Environ. Sci.* **2020,** 13, 3361–3392.

62. Maduraiveeran, G.; Sasidharan, M.; Jin, W. Earth-abundant transition metal and metal oxide nanomaterials: Synthesis and electrochemical applications. *Prog. Mater. Sci.* **2019**, 106, 100574.

63. Hwang, J.; Rao, R.R.; Giordano, L.; Katayama, Y.; Yu, Y.; Shao-Horn, Y. Perovskites in catalysis and electrocatalysis. *Science* **2017**, *358*, 751-756.

64. Chen, D.; Chen, C.; Baiyee, Z.M.; Shao, Z.; Ciucci, F. Nonstoichiometric oxides as low-cost and highly-efficient oxygen reduction/evolution catalysts for low-temperature electrochemical devices. *Chem. Rev.* **2015**, *115*, 9869-9921.

65. Xue, Y.; Sun, S.; Wang, Q.; Dong, Z.; Liu, Z. Transition metal oxide-based oxygen reduction reaction electrocatalysts for energy conversion systems with aqueous electrolytes. *J. Mater. Chem. A* **2018**, *6*, 10595-10626.

66. Anantharaj, S.; Kundu, S. Do the evaluation parameters reflect intrinsic activity of electrocatalysts in electrochemical water splitting?, *ACS Energy Letters* **2019**, *4*(6), 1260-1264.

67. Zhang, K.; Zou, R. Advanced Transition Metal-Based OER Electrocatalysts: Current status, opportunities, and challenges, *Small* **2021**, *17(37)*. 2100129.

68. Li, L.; Tian, T.; Jiang, J.; Ai, L. Hierarchically porous Co_3O_4 architectures with honeycomb-like structures for efficient oxygen generation from electrochemical water splitting. *J. Power Sources* **2015**, *294*, 103-111.

69. Ramírez, A.; Hillebrand, P.; Stellmach, D.; May, M.M.; Bogdanoff, P.; Fiechter, S. Evaluation of MnOx, Mn_2O_3 and Mn_3O_4 electrodeposited films for the oxygen evolution reaction of water. *J. Phys. Chem. C.* **2014**, *118*, 14073-14081.

70. Chen, Y.Y.; Zhang, Y.; Zhang, X.; Tang, T.; Luo, H.; Niu, S.; Dai, Z.H.; Wan, L.J.; Hu, J.S. Self-templated fabrication of $MoNi_4/MoO_{3-x}$ nanorod arrays with dual active components for highly efficient hydrogen evolution. *Adv. Mater.* **2017**, *29*, 1703311.

71. Wu, R.; Xiao, B.; Gao, Q.; Zheng, Y.R.; Zheng, X.S.; Zhu, J.F.; Gao, M.R.; Yu, S.H. A janus nickel cobalt phosphide catalyst for high-efficiency neutral-pH water splitting. *Angew. Chem.* **2018**, *130*, 15671-15675.

72. Song, F.; Bai, L.; Moysiadou, A.; Lee, S.; Hu, C.; Liardet, L.; Hu, X. Transition metal oxides as electrocatalysts for the oxygen evolution reaction in alkaline solutions: an application-inspired renaissance. *J. Am. Chem. Soc.* **2018**, *140*, 7748-7759.

73. Gür, T.M. Review of electrical energy storage technologies, materials and systems: challenges and prospects for large-scale grid storage. *Energ Environ Sci.* **2018**, *11*, 2696-2767.

74. Zhang, Y.; Fu, Q.; Song, B.; Xu, P. Regulation strategy of transition metal oxide-based electrocatalysts for enhanced oxygen evolution reaction. *Acc. Mater. Res.* **2022**, *3*, 1088-1100.

75. Ling, T.; Yan, D.Y.; Jiao, Y.; Wang, H.; Zheng, Y., Zheng, X., Mao, J., Du, X.W., Hu, Z., Jaroniec, M. and Qiao, S.Z. Engineering surface atomic structure of single-crystal cobalt (II) oxide nanorods for superior electrocatalysis. *Nat. Commun.* **2016**, *7*, 12876.

76. Hu, C.; Wang, X.; Yao, T.; Gao, T.; Han, J.; Zhang, X.; Zhang, Y.; Xu, P.; Song, B. Enhanced electrocatalytic oxygen evolution activity by tuning both the oxygen vacancy and orbital occupancy of B-site metal cation in $NdNiO_3$. *Adv. Funct. Mater.* **2019**, *29*, 1902449.

77. Peng, L.; Yang, N.; Yang, Y.; Wang, Q.; Xie, X.; Sun-Waterhouse, D.; Shang, L.; Zhang, T.; Waterhouse, G.I. Atomic cation-vacancy engineering of NiFe-layered double hydroxides for improved activity and stability towards the oxygen evolution reaction. *Angew. Chem. International Edition* **2021**, *60*, 24612-24619.

78. Chen, D.; Qiao, M.; Lu, Y.R.; Hao, L.; Liu, D.; Dong, C.L.; Li, Y.; Wang, S. Preferential cation vacancies in perovskite hydroxide for the oxygen evolution reaction. *Angew. Chem. International Edition* **2018**, *57*, 8691-8696.

79. Kim, M.; Park, J.; Kang, M.; Kim, J.Y.; Lee, S.W. Toward efficient electrocatalytic oxygen evolution: emerging opportunities with metallic pyrochlore oxides for electrocatalysts and conductive supports. *ACS Cent. Sci.* **2020**, *6*, 880-891.

80. Liu, Y.; Ying, Y.; Fei, L.; Liu, Y.; Hu, Q.; Zhang, G.; Pang, S.Y.; Lu, W.; Mak, C.L., Luo, X.; Zhou, L. Valence engineering via selective atomic substitution on tetrahedral sites in spinel oxide for highly enhanced oxygen evolution catalysis. *J. Am. Chem. Soc.* **2019**, *141*, 8136-8145.

81. Retuerto, M.; Pascual, L.; Calle-Vallejo, F.; Ferrer, P.; Gianolio, D.; Pereira, A.G.; García, Á.; Torrero, J.; Fernández-Díaz, M.T.; Bencok, P.; Peña, M.A. Na-doped ruthenium perovskite electrocatalysts with improved oxygen evolution activity and durability in acidic media. *Nature Commun.* **2019**, *10*, 2041.

82. Xu, X.; Su, C.; Zhou, W.; Zhu, Y.; Chen, Y.; Shao, Z. Co-doping strategy for developing perovskite oxides as highly efficient electrocatalysts for oxygen evolution reaction. *Adv. Sci.* **2019**, *3*, 1500187.

83. Su, C.; Wang, W.; Chen, Y.; Yang, G.; Xu, X.; Tadé, M.O.; Shao, Z. $SrCo_{0.9}Ti_{0.1}O_{3-\delta}$ as a new electrocatalyst for the oxygen evolution reaction in alkaline electrolyte with stable performance. *ACS Appl. Mater. Interfaces* **2015**, *7*, 17663-17670.

84. Liu, X.; Hong, R.; Tian, C. Tolerance factor and the stability discussion of ABO_3-type ilmenite. *J. Mater. Sci.: Mater. Electron.* **2009**, *20*, 323-327.

85. Qi, W.; Mattursun, A.; Gao, M.; Hushur, A.; Zhang, H. Lattice dynamics of $NiTiO_3$ under high pressure: Raman evidence under two pressure-transmitting mediums. *Results Phys.* **2022**, *43*, 106114.

86. Lin, Y.J.; Chang, Y.H.; Yang, W.D.; Tsai, B.S. Synthesis and characterization of ilmenite $NiTiO_3$ and $CoTiO_3$ prepared by a modified Pechini method. *J. Non-Cryst. Solids* **2006**, *352*, 789-794.

87. Tursun, R.; Su, Y.C.; Yu, Q.S.; Tan, J.; Hu, T.; Luo, Z.B.; Zhang, J. Effect of doping on the structural, magnetic, and ferroelectric properties of $Ni_{1-x}A_xTiO_3$ (A = Mn, Fe, Co, Cu, Zn; x= 0, 0.05, and 0.1). *J. Alloys Compd.* **2019**, *773*, 288-298.

88. Barman, S.; Sahu, P.P. $NiTiO_3$ Perovskite Nanoparticles for Highly Durable Hydrogen and Oxygen Evolution in Water Splitting. *IEEE Global Conference on Computing, Power and Communication Technologies (GlobConPT)*, **2022**, *September*, 1-3.

89. Guiet, A.; Huan, T.N.; Payen, C.; Porcher, F.; Mougel, V., Fontecave, M.; Corbel, G. Copper-substituted $NiTiO_3$ ilmenite-type materials for oxygen evolution reaction. *ACS Appl. Mater. Iinterfaces* **2019**, *11*, 31038-31048.

90. Manoharan, R.; Goodenough, J.B. Hydrogen Evolution on $Sr_xNbO_{3-\delta}$ ($0.7 \leq x \leq 0.95$) in Acid. *J. Electrochem. Soc.* **1990**, *137*, 910.

91. Goodenough, J.B.; Manoharan, R.; Paranthaman, M. Surface protonation and electrochemical activity of oxides in aqueous solution. *Journal Am. Chem. Soc.* **1990**, *112*, 2076-2082.

92. Xu, X.; Chen, Y.; Zhou, W.; Zhu, Z.; Su, C.; Liu, M.; Shao, Z. A perovskite electrocatalyst for efficient hydrogen evolution reaction. *Adv. Mater.* **2016**, *28*, 6442-6448.

93. Zhu, Y.; Zhou, W.; Zhong, Y.; Bu, Y.; Chen, X.; Zhong, Q.; Liu, M. Shao, Z. A perovskite nanorod as bifunctional electrocatalyst for overall water splitting. *Adv. Energy Mater.* **2017**, *7*, 1602122.

94. Hua, B.; Li, M.; Zhang, Y.Q.; Sun, Y.F.; Luo, J.L. All-in-one perovskite catalyst: smart controls of architecture and composition toward enhanced oxygen/hydrogen evolution reactions. *Adv. Energy Mater.* **2017**, *7*, 1700666.

95. Fabbri, E.; Habereder, A.; Waltar, K.; Kötz, R.; Schmidt, T.J. Developments and perspectives of oxide-based catalysts for the oxygen evolution reaction. *Catal. Sci. Techno.* **2014**, *4*, 3800-3821.

96. Gao, Z.; Mogni, L.V.; Miller, E.C.; Railsback, J.G.; Barnett, S.A. A perspective on low-temperature solid oxide fuel cells. *Energy Environ. Sci.* **2016**, *9*, 1602-1644.

97. Xu, X.; Zhong, Y.; Shao, Z. Double perovskites in catalysis, electrocatalysis, and photo (electro) catalysis. *Trends Chem.* **2019**, *1*, 410-424.

98. Guan, D.; Zhou, J.; Hu, Z.; Zhou, W.; Xu, X.; Zhong, Y.; Liu, B.; Chen, Y.; Xu, M.; Lin, H.J.; Chen, C.T. Searching general sufficient-and-necessary conditions for ultrafast hydrogen-evolving electrocatalysis. *Adv. Funct. Mater.* **2019**, *29*, 1900704.

99. Guan, D.; Zhou, J.; Huang, Y.C.; Dong, C.L.; Wang, J.Q.; Zhou, W.; Shao, Z. Screening highly active perovskites for hydrogen-evolving reaction via unifying ionic electronegativity descriptor. *Nat. Commun.* **2019**, *10*, 3755.

100. Chen, D.; Chen, C.; Baiyee, Z.M.; Shao, Z.; Ciucci, F. Nonstoichiometric oxides as low-cost and highly-efficient oxygen reduction/evolution catalysts for low-temperature electrochemical devices. *Chem. Rev.* **2015**, *115*, 9869-9921.

101. Zhu, Y.; Lin, Q.; Hu, Z.; Chen, Y.; Yin, Y.; Tahini, H.A.; Lin, H.J.; Chen, C.T.; Zhang, X.; Shao, Z.; Wang, H. Self-assembled ruddlesden–popper/perovskite hybrid with lattice-oxygen activation as a superior oxygen evolution electrocatalyst. *Small* **2020**, *16*, 2001204.

102. Zhu, Y.; Tahini, H.A.; Hu, Z.; Dai, J.; Chen, Y.; Sun, H.; Zhou, W.; Liu, M.; Smith, S.C.; Wang, H.; Shao, Z. Unusual synergistic effect in layered Ruddlesden− Popper oxide enables ultrafast hydrogen evolution. *Nat. Commun.* **2019**, *10*, 149.

103. Xu, X.; Pan, Y.; Zhong, Y.; Ran, R.; Shao, Z. Ruddlesden–Popper perovskites in electrocatalysis. *Mater. Horiz.* **2020**, *7*, 2519-2565.

104. Shi, Y.; Zhang, B. 'Correction: Recent advances in transition metal phosphide nanomaterials: synthesis and applications in hydrogen evolution reaction,' *Chem. Soc. Rev.* **2016**, *45*, 1781.

105. Anantharaj, S.; Karthick, K.; Kundu, S. Evolution of layered double hydroxides (LDH) as high-performance water oxidation electrocatalysts: A review with insights on structure, activity and mechanism *Mater. Today Energy* **2017**, *6*, 1–26.

106. Callejas, J.F.; McEnaney, J.M.; Read, C.G.; Crompton, J.C.; Biacchi, A.J.; Popczun, E.J.; Gordon, T.R.; Lewis, N.S.; Schaak, R.E. Electrocatalytic and Photocatalytic Hydrogen Production from Acidic and Neutral-pH Aqueous Solutions Using Iron Phosphide Nanoparticles *ACS Nano* **2014**, *8*, 11101–11107.

107. Tang, C.; Wang, H. S.; Wang, H. F.; Zhang, Q.; Tian, G. L.; Nie, J. Q.; Wei, F. Spatially confined hybridization of nanometer-sized NiFe hydroxides into nitrogen-doped graphene frameworks leading to superior oxygen evolution reactivity. *Adv. Mater* **2015**, *27*, 4516-4522.

108. Fabbri, E.; Habereder, A.; Waltar, K.; Kötz, R.; Schmidt, T.J.; Developments and perspectives of oxide-based catalysts for the oxygen evolution reaction *Catal. Sci. Technol.* **2014**, *4*, 3800–3821.

109. Bockris, J.M.; Potter, E.C. The mechanism of the cathodic hydrogen evolution reaction. *J. Electrochem. Soc.* **1952**, *99*, 169.

110. Reier, T.; Nong, H.N.; Teschner, D.; Schlögl, R.; Strasser, P. Electrocatalytic oxygen evolution reaction in acidic environments – reaction mechanisms and catalysts *Adv. Energy Mater.* **2016**, *7*. 1601275

111. Anantharaj, S.; Ede, S.R.; Sakthikumar, K.; Karthick, K.; Mishra, S.; Kundu, S.; Recent Trends and Perspectives in Electrochemical Water Splitting with an Emphasis on Sulfide, Selenide and Phosphide Catalysts of Fe, Co, and Ni: A Review *ACS Catal.* **2016**, *6*, 8069–8097.

112. Wei, C.; Sun, S.; Mandler, D.; Wang, X.; Qiao, S.Z.; Xu, Z.J. Approaches for measuring the surface areas of metal oxide electrocatalysts for determining their intrinsic electrocatalytic activity *Chemical Soc. Rev.* **2019**, *48*, 2518–2534.

113. Trasatti, S.; Petrii, O.A. Real surface area measurements in electrochemistry. *Pure Appl. Chem.* **1991**, *63*, 711-734.

114. Orazem, M.E.; Tribollet, B. Electrochemical impedance spectroscopy. *New Jersey* **2008** *1*, 383-389.

115. Lukowski, M.A.; Daniel, A.S.; Meng, F.; Forticaux, A.; Li, L.; Jin, S. Enhanced Hydrogen Evolution Catalysis from Chemically Exfoliated Metallic MoS_2 Nanosheets,' *J. Am. Chem. Soc.* **2013**, *135*, 10274–10277.

116. McCrory, C.C.; Jung, S.; Peters, J.C.; Jaramillo, T.F.; Benchmarking heterogeneous electrocatalysts for the oxygen evolution reaction *J. Am. Chem. Soc.* **2013**, *135*, 16977–16987.

117. Anantharaj, S.; Ede, S.R.; Karthick, K.; Sankar, S.S.; Sangeetha, K.; Karthik, P.E.; Kundu, S. Precision and correctness in the evaluation of electrocatalytic water splitting: revisiting activity parameters with a critical assessment *Energy Environ. Sci.* **2018**, *11*, 744–771.

118. Kumar, T.N.; Sivabalan, S.; Chandrasekaran, N.; Phani, K.L. Synergism between polyurethane and polydopamine in the synthesis of Ni–Fe alloy monoliths *Chem. Comm.* **2014**, *51*, 1922–1925.

119. Anantharaj, S.; Jayachandran, M.; Kundu, S. Unprotected and interconnected Ru0 nano-chain networks: advantages of unprotected surfaces in catalysis and electrocatalysis *Chemical Sci.* **2016**, *7*, 3188–3205.

120. Shi, Y.; Zhang, B. Recent advances in transition metal phosphide nanomaterials: synthesis and applications in hydrogen evolution reaction. *Chem. Soc. Rev.* **2016**, *45*, 1529-1541.

121. Anantharaj, S.; Karthik, P.E.; Kundu, S. Petal-like hierarchical array of ultrathin $Ni(OH)_2$ nanosheets decorated with $Ni(OH)_2$ nanoburls; a highly efficient OER electrocatalyst *Catalysis Sci. Technol.* **2017**, *7*, 882–893.

122. Stratton, S.M.; Zhang, S.; Montemore, M.M. Addressing complexity in catalyst design: From volcanos and scaling to more sophisticated design strategies *Surf. Sci. Rep.* **2023**, *78*, 100597.

123. Gao, M.; Sheng, W.; Zhuang, Z.; Fang, Q.; Gu, S.; Jiang, J.; Yan, Y. Efficient water oxidation using nanostructured α-nickel-hydroxide as an electrocatalyst *J. Am. Chem. Soc.* **2014**, *136*, 7077-7084.

124. Wei, C.; Sun, S.; Mandler, D.; Wang, X.; Qiao, S.Z.; Xu, Z.J. Approaches for measuring the surface areas of metal oxide electrocatalysts for determining their intrinsic electrocatalytic activity *Chem. Soc. Rev.* **2019**, *48*, 2518–2534.

125. Gao, M.; Sheng, W.; Zhuang, Z.; Fang, Q.; Gu, S.; Jiang, J.; Yan, Y. Efficient water oxidation using nanostructured α-nickel-hydroxide as an electrocatalyst *J. Am. Chem. Soc.* **2014**, *136*, 7077-7084.

126. Subbaraman, R.; Tripkovic, D.; Chang, K.C.; Strmcnik, D.; Paulikas, A.P.; Hirunsit, P.; Chan, M.; Greeley, J.; Stamenkovic, V.; Markovic, N.M. Trends in activity for the water electrolyser reactions on 3d M(Ni,Co,Fe,Mn) hydr(oxy)oxide catalysts *Nat. Mater.* **2012**, *11*, 550–557.

127. Anantharaj, S.; Kennedy, J.; Kundu, S. Microwave-initiated facile formation of Ni_3Se_4 nanoassemblies for enhanced and stable water splitting in neutral and alkaline media. *ACS Appl. Mater. Interfaces* **2017**, *9*, 8714-8728.

128. Anantharaj, S.; Reddy, P. N.; Kundu, S. Core-oxidized amorphous cobalt phosphide nanostructures: an advanced and highly efficient oxygen evolution catalyst. *Inorg. Chem.* **2017**, *56*, 1742-1756.

129. Anantharaj, S.; Karthik, P.E.; Subramanian, B.; Kundu, S. Pt nanoparticle anchored molecular self-assemblies of DNA: an extremely stable and efficient HER electrocatalyst with ultralow Pt content. *ACS Catal.* **2016**, *6*, 4660-4672.